[5]

A COMPARISON OF ARM AND TRM IN MAGNETITE

SHAUL LEVI

Department of Geology and Geophysics, University of Minnesota, Minneapolis, Minn. 55455 (USA)

and

RONALD T. MERRILL

Geophysics Program and Oceanography Department, University of Washington, Seattle, Wash. 98195 (USA)

Experiments comparing anhysteretic remanence (ARM) and thermoremanence (TRM) in samples containing natural and synthetic magnetite, whose mean particle sizes range from single domain to multidomain, show that ARM and TRM are very similar (but not identical) in their stabilities with respect to alternating field (AF) demagnetization, temperature cycles in zero field to below magnetite's isotropic temperature near $130°K$, and stability with respect to spontaneous decay in zero field. Therefore, for magnetites, ARM can be used to model (with reasonable success) these stability properties of TRM. The field dependence of the acquisition of ARM and TRM shows that the low field susceptibility ratio, x_{ARM}/x_{TRM}, has a particle size dependence, increasing from 0.1 for certain submicron particles to 2.0 for large multidomain crystals. Even for samples whose remanence is predominantly carried by submicron particles x_{ARM}/x_{TRM} is highly variable, $0.11 \leqslant x_{ARM}/x_{TRM} \leqslant 0.50$. Therefore, ARM paleointensity methods which do not take into account the large variability in and the particle size dependence of x_{ARM}/x_{TRM} are subject to order-of-magnitude uncertainties.

1. Introduction

Anhysteretic remanent magnetization (ARM), as defined in this paper, is the magnetization acquired when the amplitude of an alternating field, H, is reduced from its peak value to zero in the presence of a direct magnetic field, h, whose direction and intensity are constant. The ARM is measured when both h and H equal zero.

ARM was studied as early as 1885 by J.A. Ewing [7]. Further experimental and theoretical studies [1–7] have shown that for a given direct field, h, ARM was much more intense, had substantially greater initial susceptibility, and had greater stability than isothermal remanent magnetization (IRM). For these reasons, ARM is sometimes called "ideal" magnetization (especially by the Soviet rock magnetists). The contrast between ARM and IRM of the above studies was qualitatively explained by the use

of Preisach diagrams [8]. Recent work on ARM has been spurred by its similarity to magnetic recording processes [9,10]. With the possible exception of remanence produced by lightning, ARM does not occur in nature. ARM is occasionally a source of noise in paleomagnetic studies when it is inadvertently produced during alternating field (AF) demagnetization experiments.

Previous work has suggested that the properties of ARM are very similar to those of thermal remanent magnetization (TRM). In particular, it has been shown [7] that ARM and TRM have comparable stabilities against alternating field and thermal demagnetization and that ARM intensity is linearly proportional to a *weak* inducing field. Subsequent studies have expanded the list of similarities between ARM and TRM to include the observation that ARM obeys the additivity law for partial ARMs [11,12].

Because of the many similarities between ARM and

TRM, several workers have substituted ARM for TRM in rock magnetic studies to eliminate chemical alteration effects that could arise during the heating of samples. For example, with the exception of a few control experiments that used TRM, ARM was used in the oxidation experiments of Johnson and Merrill [13–15]. ARM has been used in analyses of deep-sea and lake sediments to gain insight concerning the origin of the remanence and variations in its relative intensity [16,17]. ARM has also been used in some absolute paleointensity methods [18–21].

Although there are substantial data supporting the similarity of ARM properties to those of TRM, one suspects that some differences must exist simply because of the very different processes by which a sample acquires an ARM versus a TRM. For example, magnetic properties are very temperature-dependent and therefore vary during TRM acquisition, while ARM acquisition is an isothermal process. Because of this and because of the increased use of ARM, this study was undertaken to see how far the ARM-TRM analogy can be carried and where their properties diverge. We report here on experiments that compare ARM properties with TRM properties for a wide variety of magnetite samples. It is, to the best of our knowledge, the first systematic study which compares TRM and ARM properties of the same sample.

2. Magnetite samples and experimental procedures

The samples used in these experiments were described in another paper [22] and will not be discussed in detail here. The second column of Table 1 summarizes the particle sizes and many of their properties. It is important to emphasize that the magnetite samples do not come from the same source; in fact, some are synthetic and some are from naturally occurring crystals. One of the most important differences that exist between synthetic magnetites versus natural magnetites is that the former are typically substantially oxidized along the solid solution between magnetite and maghemite [23], while the latter contain little maghemite unless substantial oxidation occurred after the sample had cooled or during the very late cooling stages [24]. For this reason, before conducting the experiments of this study, all our samples were heated to 600°C, a temperature that exceeds the Curie

temperature of magnetite (~580°C), in an atmosphere that reduced maghemite to magnetite. In some cases such heating resulted in other changes as well, such as particle growth due to sintering. Although the details of these experiments are described in a different paper [22], it is important to emphasize that *all* the properties given in Table 1 are for samples which have been given several TRMs by heating to 600°C until the TRM intensity and its stability, as measured by AF demagnetization, were reproducible to within 5%.

ARM and TRM properties are compared in the same sample. Only one heating (that of a total thermal demagnetization at about 590°C) separated the ARM and TRM comparisons. Magnetic measurements were made with a Schonstedt spinner magnetometer. AF demagnetization was conducted in a low-field environment using a 4-axis tumbler system. Low-temperature experiments were conducted inside a non-magnetic space ($\pm 50\gamma = \pm 50$ nT) with automatic feedback. High-field magnetization versus temperature experiments were conducted using a Princeton Applied Research vibrating sample magnetometer. ARM was imparted using small Helmholtz coils which fit around the sample to provide the small steady field. The sample and Helmholtz coils both fit inside our AF demagnetization solenoid, and an ARM was given by peak AF fields between 1000 and 2000 Oe (1000 and 2000×10^{-4} T), depending on the alternating field required to produce saturation ARM for a particular direct field. Sample 11 was the only sample of this study whose ARM was not saturated with a 2000-Oe alternating field for the biasing fields which were used. Sample 11 was approximately within 10% of saturation.

All the ARMs of this paper were produced by direct fields which were always parallel to the axis of the alternating field ($h \parallel H$). (Rimbert [7] showed that ARM is acquired parallel to h, even when h is perpendicular to H. However, when $h \parallel H$ the ARM is about 1.4 times as intense as when $h \perp H$.)

3. Comparison of the stability of ARM and TRM as measured by AF demagnetization

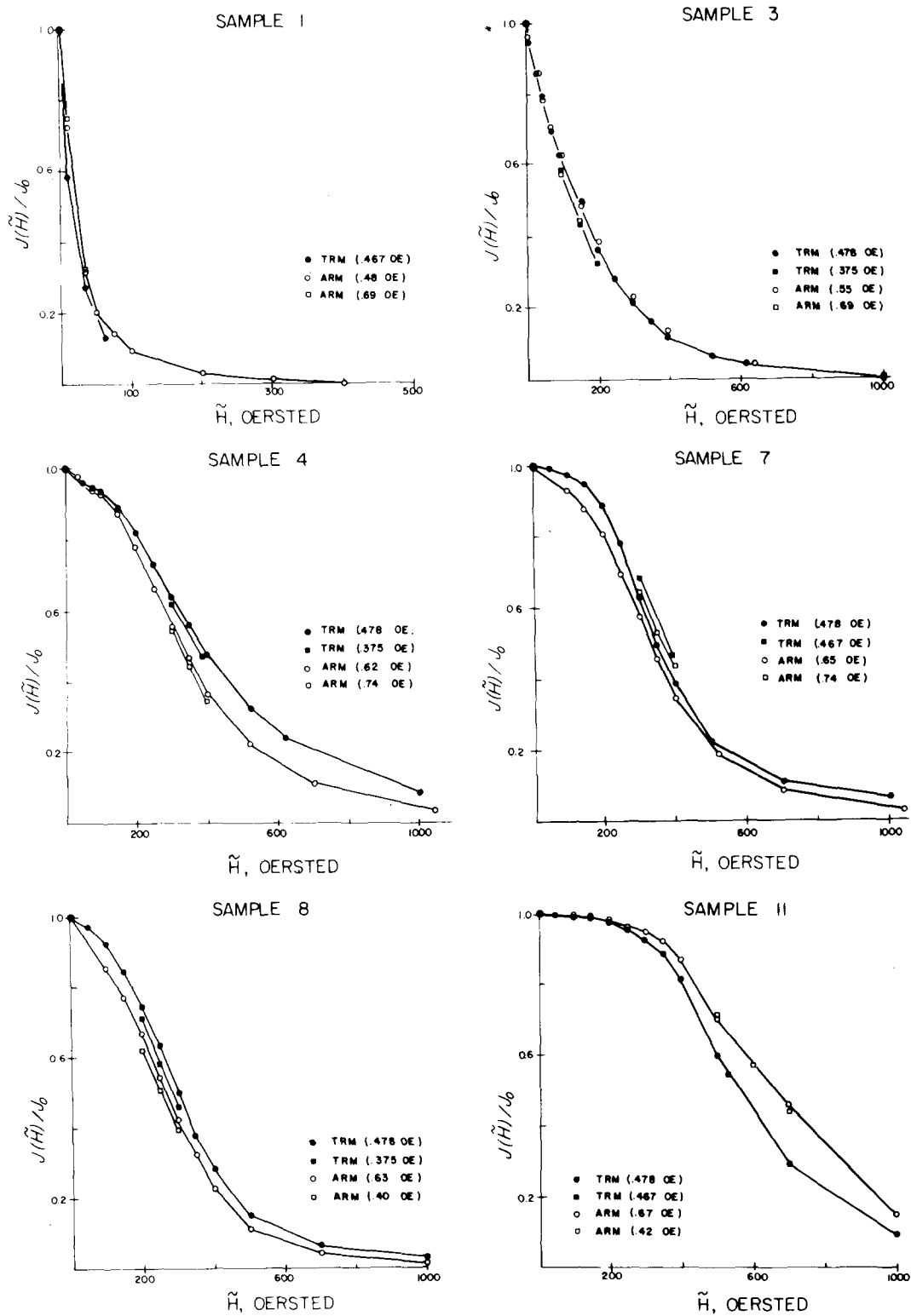AF demagnetization curves of ARM and TRM exhibit very similar shapes for all samples. TRMs

Fig. 1. Normalized AF demagnetization curves of ARM (open symbols) and TRM (solid symbols). The circles represent the first sequence of AF demagnetization experiments. Squares represent the second sequence of AF demagnetizations.

174

TABLE 1

Comparison of TRM and ARM properties in magnetite

SAMPLE NUMBER	DESCRIPTION OF MAGNETITE PARTICLES	$H_{1/2}$ (OERSTED) TRM	$H_{1/2}$ (OERSTED) ARM	LOW TEMPERATURE CYCLES (NORMALIZED) TRM	LOW TEMPERATURE CYCLES (NORMALIZED) ARM	SPONTANEOUS DECAY t=24HOURS (NORMALIZED) TRM	SPONTANEOUS DECAY t=24HOURS (NORMALIZED) ARM	χ_{ARM}/χ_{TRM}	MEAN TRM h = 0.50 OE $\times 10^{-3}$ gauss
0	NATURAL CRYSTAL EUHEDRAL 6.379 gm	12±3	27±3 / 27±3	0.136 / 0.110 / 0.106	-.052 / 0.116 / 0.136	0.926 ±.013	0.975 ±.005	2.0±.4	3.88
1	CHIP OF NATURAL CRYSTAL 3.569 gm	17±3	24±3 / 25±3	-.091 / -.092 / -.101	0.144 / 0.082 / 0.092	0.924 ±.012	0.944 ±.012	1.5±.3	8.43
2	NATUR., IRREG. $\langle d\rangle$ =2.7 μm d =150 μm MAX	82±5 / 74±5	58±5 / 49±5	0.590 / 0.465 / 0.476	0.413 / 0.386 / 0.370	0.938 ±.002	0.980 ±.004	0.64±.06	0.258
3	NATUR., IRREG. $\langle d\rangle$ =1.5 μm d =50 μm MAX	147±10 / 129±10	144±10 / 126±10	0.593 / 0.521 / 0.497	0.561 / 0.537 / 0.524	0.970 ±.005	0.995 ±.005	0.45±.04	2.32
4	NATUR., REGULAR $\langle d\rangle$ =0.3μm d = 2 μm MAX	388±10 / 373±10	330±10 / 315±10	0.936 / 0.889 / 0.822	0.929 / 0.916 / 0.913	0.990 ±.002	0.985 ±.004	0.44±.04	0.964
5	SYNTHETIC, CUBES→SPHERES $\langle d\rangle$ =0.24 μm d =0.9 μm MAX	347±10 / 347±10	337±10 / 350±10	0.945 / 0.935 / 0.929	0.980 / 0.942 / 0.932	0.992 ±.002	0.990 ±.001	0.188±.010	2.97

175

|							
6	SYNTHETIC, CUBES→SPHERES <d> =0.21 μm d =0.5 μm MAX	337±10 331±10	387±10 416±10 423±10	0.976 0.951 0.945	0.964 0.964 0.961	0.995 ±.004	1.000 ±.000	0.164±.008	1.34
7	SYNTHETIC, CUBES→SPHERES <d> =0.21 μm d =0.5 μm MAX	346±10 375±10	333±10 363±10 366±10	0.965 0.961 0.955	0.920 0.914 0.905	0.998 ±.002	0.998 ±.002	0.108±.005	14.49
8	SYNTHETIC, CUBES→SPHERES <d> =0.12 μm d =0.3 μm MAX	300±10 284±10	268±10 254±10 264±10	0.990 0.971 0.965	0.978 0.974 0.951	0.967 ±.002	0.926 ±.010	0.50±.03	1.17
9	SYNTHETIC, CUBES→SPHERES <d> =0.12 μm d =0.3 μm MAX	285±10 306±10	237±10 251±10 232±10	0.986 0.910 0.907	0.980 0.976 0.956	0.958 ±.002	0.895 ±.010	0.49±.03	1.04
10	MAGNETITE UNKNOWN SIZE AND SHAPE d < =0.5 μm	421±20	382±20 401±20	0.982 0.974 0.960	0.945 0.934 0.934	0.994 ±.012	0.993 ±.007	0.312±.015	0.0295
11	SYNTHETIC, ACICULAR AXIAL RATIO 8:1 0.35μm x 0.04 μm	565±25	672±25 656±25	1.003 0.995 0.994	0.995 0.995 0.988	0.998 ±.002	1.000 ±.002	0.238±.012	3.36
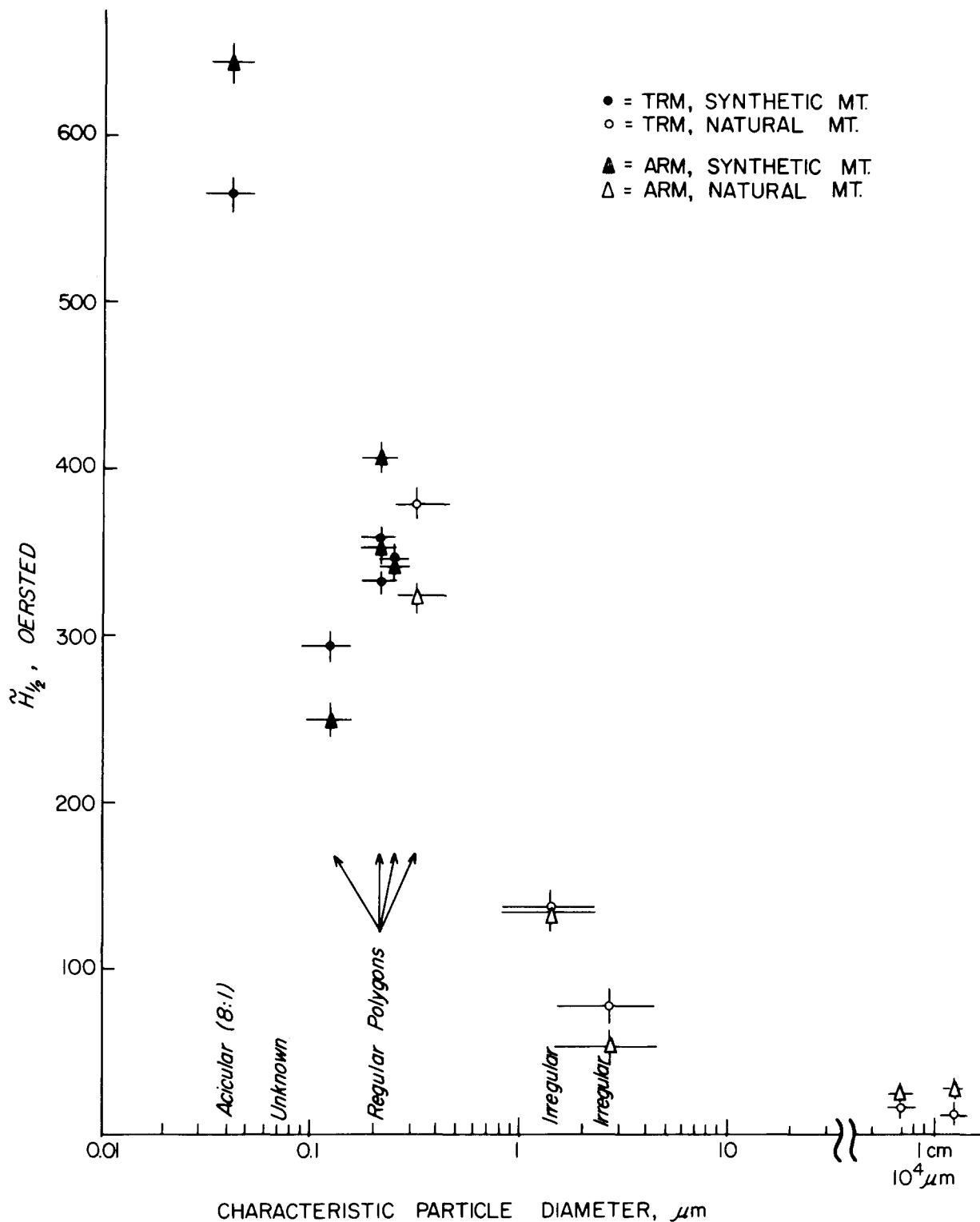
Fig. 2. A plot of $H_{1/2}$, median demagnetizing field, versus the characteristic particle diameter for ARM (triangles) and TRM (circles) for the magnetite-bearing samples. Note that $H_{1/2}$ of both ARM and TRM follows the same pattern. The uncertainties associated with the mean particle diameters are related whenever possible to the standard deviations of the particle diameters obtained from electron microscope photographs. The uncertainties associated with the $H_{1/2}$ values represent deviations from the mean of independent determinations. From right to left along the abscissa the data correspond to samples 0, 1, 2, 3, 4, 5, 6, and 7, 8 and 9, and 11.

were induced by fields between 0.3 and 0.5 Oe (1 Oe = 10^{-4} tesla), and ARMs were produced by direct fields between 0.4 and 0.7 Oe. Typical examples for six samples are shown in Fig. 1, which also includes the specific inducing fields for each sample. Since ARMs and TRMs were induced in slightly different biasing fields, we draw no conclusions concerning the differences between the stabilities of the ARM and TRM demagnetization curves, when these differences are very small.

The similarity of the AF demagnetization curves allows us to characterize them by a single parameter, which we arbitrarily choose as the median demagnetizing field, $H_{1/2}$ that alternating field for which the magnetization drops to half its initial value. To test how reliably $H_{1/2}$ could be reproduced for each sample, a limited version of the AF demagnetization experiments was repeated. Using the original data as guide, AF values were chosen to bracket $H_{1/2}$. The second sequence of AF demagnetization experiments (represented by squares in Fig. 1) was separated from the first by over twenty heatings to between 500° and 600°C. However, the ARM and TRM of this second sequence of AF demagnetization were separated only by a single heating to 590°C. By and large the results of the two AF demagnetization experiments are very similar. Although some of the $H_{1/2}$ values shifted between the two demagnetization sequences, the relationships between the ARM and TRM did not change. For samples 2, 3, and 4, whose particles were obtained by the grinding of a large magnetite crystal, the AF stabilities decrease with progressive heating, suggesting that some annealing was still occurring. For the synthetic magnetites, the effects of heating on the AF stabilities is not so regular. Despite the ambiguity introduced by the fact that the biasing fields are not equal, the results, showing that the ARM and TRM for each sample maintain the same relative stabilities for both sequences of AF demagnetization, suggest to us that differences in the demagnetization curves are due mostly to differences between ARM and TRM, rather than to differences in the biasing field.

The largest difference in the stabilities of ARM and TRM is exhibited by sample 11, for which the ARM is considerably more stable than the TRM. The difference is considered significant because it is reproducible and because sample 11 is the only sample whose ARM was not totally saturated by a 2000-Oe (2000 × 10^{-4} T) alternating field. This result suggests that some of the particles of sample 11 possess microscopic coercivities approaching theoretically predicted values for needle-shaped magnetite particles.

Values of $H_{1/2}$ are given in Table 1 and are plotted versus the mean magnetite particle size in Fig. 2. These data show the similarity of the AF stabilities of ARM and TRM in each sample, which span a broad range of particle sizes and shapes. In addition, the $H_{1/2}$ values of both ARM and TRM follow very similar particle size trends. The data for sample 10 is omitted from Fig. 2 because of the unknown size and shape distributions of its magnetite particles. For particles of equal shapes and of the same species of magnetic material the stability is expected to increase with increasing particle size within the single-domain size range [39], and the stability is known to decrease with increasing size for multidomain particles. Therefore, there should be a maximum in the stability versus particle size curve; this is consistent with the data of Fig. 2. The data of sample 11 do not fit the trend of the remaining samples because of the highly acicular shape of its magnetite particles.

4. ARM and TRM stabilities with respect to low-temperature cycles

The decay of a sample's magnetization when it is cooled in a non-magnetic space below 130°K, the magnetocrystalline anisotropy transition temperature, and subsequently heated to room temperature gives some indication of the amount of remanence controlled by the magnetocrystalline anisotropy energy [25–28]. Above 130°K the magnetocrystalline easy axes are the [111] directions, while below 130°K they are the [100] directions. The work of Ozima et al. [26] indicates that a completely annealed multidomain sample will experience a loss of remanence on cooling in a non-magnetic space below 130°K and a further loss of remanence on heating to room temperature. However, if internal stress is present, a partial recovery (termed "memory") will occur on heating the sample. This recovery appears to occur because some of the initial remanence along the [111] directions does not change direction to a nearby [100] direction on cooling through the 130°K temperature

due to the presence of magnetostrictibe anisotropy associated with the internal stress. This "pinned" remanence acts as a nucleation center for the recovery of remanence on heating [27]. On the other hand, single-domain magnetite grains exhibit very different types of behavior. Small departures from a spherical shape for a single-domain magnetite grain will cause shape anisotropy to completely dominate the other anisotropies. Therefore, a change in the magnetocrystalline anisotropy easy direction is only rarely of consequence and little loss of remanence is expected or observed when single-domain magnetite is cycled across the low-temperature transition point [27]. The behavior of pseudo-single-domain grains is somewhat harder to predict because of uncertainties in just what constitutes a "pseudo-single-domain grain". If such grains can be represented by part or all of a domain wall, as is done in one of the models [29, p. 60], then the shape anisotropy cannot be reduced by much more than $2/\pi$ of a uniformly magnetized grain. Therefore, pseudo-single-domain grains should also exhibit only a very small loss of remanence when cycled through a low-temperature transition (although this loss should be somewhat larger than the very small loss exhibited by single-domain grains). The loss of remanence continues with each successive low-temperature cycle, although the magnitude of the loss associated with a given cycle decreases with successive cycles [28].

All these expectations are consistent with the low-temperature data given in Table 1. (This table also gives the median destructive alternating field, the results of a storage test, and the ratio of the weak field ARM susceptibility to TRM susceptibility, which will be discussed later.) The largest change in the amount of remanence loss after three low-temperature cycles occurs between samples with mean diameter sizes of 0.31 and 1.5 μm, which might suggest that this is roughly the upper limit that pseudo-single-domain grains filled by a wall can carry the remanence. A second decrease in remanence occurs somewhere above 2.7 μm but less than the very large magnetite grains. This change may be gradual, reflecting the fact that larger grains contain more domains, or it may be more sharp. Although at present we do not understand the large differences in the estimates for the upper size limits of pseudo-single-domain particles of 15 μm [30,31] and our own results, differ-

ences in chemistry, shape, and/or magnetic interactions may be partly responsible. In addition, it has been shown [32] (see also Table 1, column 2) that sample 2 (3) whose mean particle size is 2.7 μm (1.5 μm) contains particles as large as 150 μm (50 μm); this underlines the importance of more complete descriptions of particle sizes and shapes when they are critical in an experiment. Alternatively, one type of pseudo-single-domain grain may be dominant in our samples and another type dominant in those of the Toronto scientists [30,31]. Indeed, it has been suggested [29] that there are at least two types of pseudo-single-domain grains, and Schmidt [42] has suggested another type by showing that grains with only a couple of domains can behave substantially differently than grains with several domains.

Generally, low-temperature cycles appear to affect ARM and TRM in a similar fashion, as can be seen in Table 1. However, some differences do exist, particularly in the samples with the larger particles. The most obvious difference occurs in sample 1, in which the TRM undergoes a self-reversal after a low-temperature cycle, while the ARM does not. (Self-reversals have been previously observed in similar samples, and this behavior has been adequately explained [26].) This difference between ARM and TRM in sample 1 is repeatable and indicates that sometimes ARM and TRM affect the sample in different ways, producing distinct remanences. On the other hand, the difference between ARM and TRM for the low-temperature behavior of sample 1 may not be very significant, because samples 0 and 1 are magnetically very "soft" and because single crystals are notoriously difficult to totally demagnetize.

5. Stability of ARM and TRM with respect to spontaneous decay

Another stability index of a particular remanence is the rate at which it decays when it is stored in zero field. In Table 1 are the results comparing the spontaneous decay of ARM and TRM, after storage in zero field at T_R for 24 hours. The uncertainties associated with the values in Table 1 are deviations from the mean of two separate and independent spontaneous decay determinations. The TRMs were produced in fields of 0.47 and 0.48 Oe (0.47 and 0.48 × 10^{-4} T). The

ARMs were produced by biasing fields of 0.42 and 0.65 Oe (0.42 and 0.65×10^{-4} T). For this limited range of biasing fields there is no apparent field dependence of the spontaneous decay. The data show that the spontaneous decay of our magnetite samples is much less sensitive to particle sizes than both the stabilities with respect to alternating fields and with respect to low-temperature cycles. ARM and TRM have similar stabilities with respect to spontaneous decay. For samples 0, 1, 2, and 3 the ARM is somewhat more stable, and for samples 8 and 9 the TRM is more stable. For the remaining samples the ARM and TRM stabilities are indistinguishable.

6. The ratio of ARM to TRM and paleointensity studies

The determination of the intensity ratio of ARM to TRM, J_{ARM}/J_{TRM}, is important to the understanding of the origins of ARM and TRM and to some paleointensity work. Theoretical considerations [33] indicate that this ratio should never be greater than 1. The ARM paleointensity technique [19] which has been used on lunar samples may yield erroneous results if the $J_{ARM}/_{TRM}$ ratio for a constant inducing field varies greatly between rocks.

Fig. 3 gives the value for the remanent magnetization, J, for both ARM and TRM for different inducing fields. With the exception of the largest field (1.8 Oe $= 1.8 \times 10^{-4}$ T) for some of the samples with the smallest grain sizes, both the ARM and TRM acquisition appear to be linear with field strength, as expected from the theory for small inducing fields [34]. Using the linear portion, we can obtain χ_{ARM}/χ_{TRM}, the ratio of apparent susceptibilities of ARM to TRM. Note that this ratio will be identical to the intensity ratio, J_{ARM}/J_{TRM}, when the same weak inducing field is used for the ARM and TRM. We see that for the multidomain grains the ratio χ_{ARM}/χ_{TRM} appears to be greater than 1, in apparent contradiction with the theory of Gillingham and Stacey [33]. Moreover, this ratio can vary by more than an order of magnitude (from 2.0 for sample 0 to 0.108 for sample 7, Table 1). Therefore ARM paleointensity methods which fail to take into account the large variability in, and the particle size dependence of, χ_{ARM}/χ_{TRM} are subject to order-of-magnitude uncertainties. Even

for the samples whose remanence is dominated by submicron particles, the χ_{ARM}/χ_{TRM} ratio varies by a factor of 5 (compare the data of samples 7 and 8 in Table 1). In addition to this study, χ_{ARM}/χ_{TRM} ratios substantially less than unity have also been reported in [43] for equidimensional submicron magnetite particles and in [12] for acicular single-domain magnetite particles.

Although differences in the magnetic particles, sample preparation and experimental procedure make it difficult to make meaningful comparisons with the results of others, we find it instructive to make certain selective comparisons. In particular, our sample 11 appears to be very similar to sample 4 of Dunlop and West [12] for which $\chi_{ARM}/\chi_{TRM} = 0.182$ (in a 1-Oe field), which is very similar to 0.238, the susceptibility ratio of sample 11.

Banerjee and Mellema [20] report a study of highly acicular (axial ratio 10 : 1) submicron CrO_2 particles which are predominantly single domain, whose microscopic coercivity is determined by their shape anisotropy. The room temperature saturation magnetization, $J_S(T_R)$, of these CrO_2 particles is 87 emu/g, very similar to magnetite's 93 emu/g. The Curie point of CrO_2 is 128°C, in contrast with magnetite's 580°C. A value of $\chi_{ARM}/\chi_{TRM} = 0.217$ was obtained for a sample containing 1% CrO_2 powder dispersed in a non-magnetic matrix [20]. The similarity of χ_{ARM}/χ_{TRM} of both the CrO_2 sample and our magnetite sample 11, both containing acicular single-domain particles, suggests that the *temperature difference* between the blocking of TRM and the production of ARM is much less crucial in determining χ_{ARM}/χ_{TRM} than the *contrast in the particles' spontaneous magnetization* at the temperatures of TRM blocking and the production of ARM, respectively.

7. Magnetic interactions

Magnetic interactions are commonly thought to play an important role in ARM. For example, ARM's finite susceptibility has often been attributed to magnetic interactions [35–38]. Magnetic interactions have also been invoked [12] to explain the deviation of the J_{TRM} versus h curves from the theoretically predicted hyperbolic tangent behavior. Jaep [34] con-
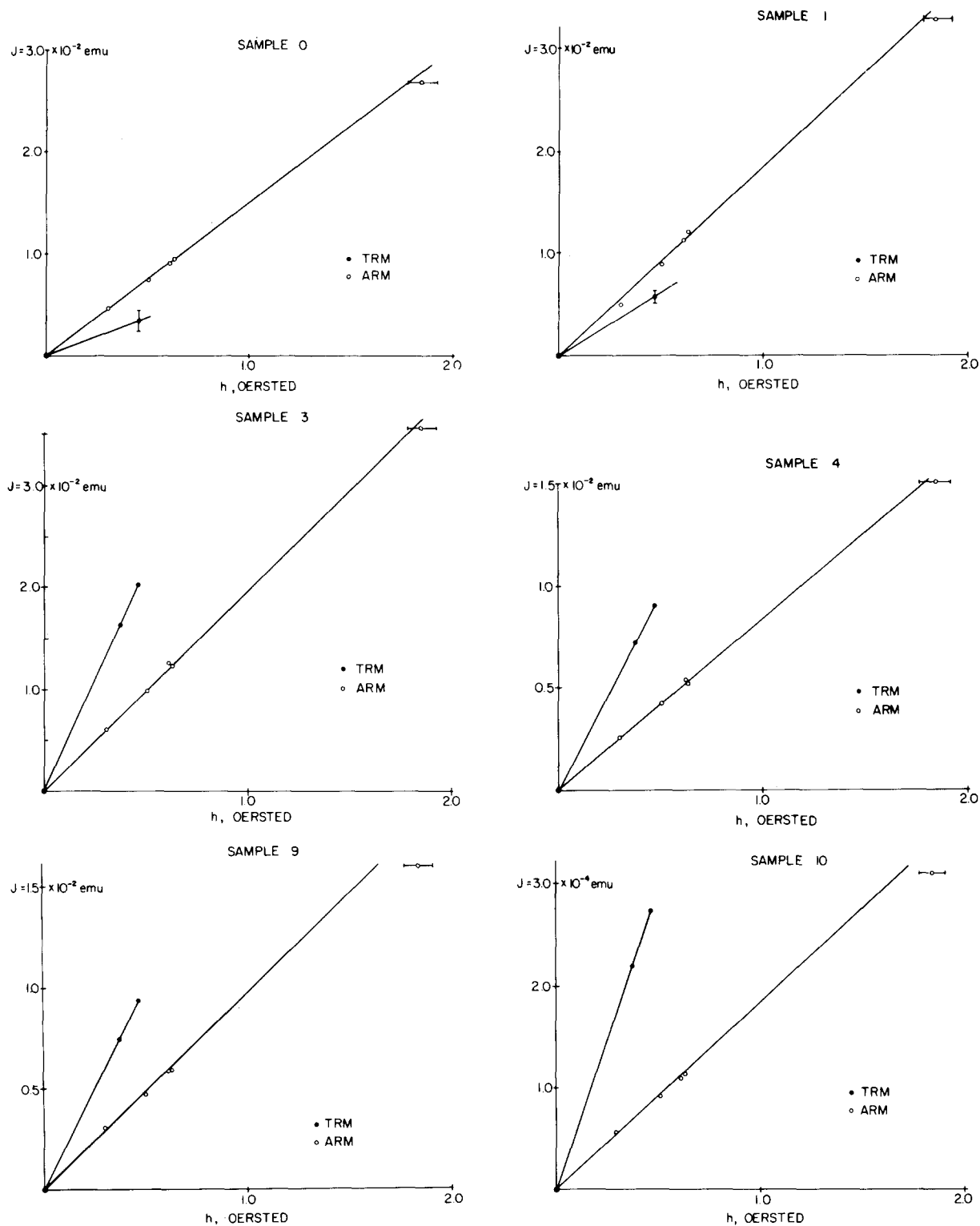
Fig. 3. Acquisition of ARM (open circles) and TRM (closed circles) versus biasing fields. ARMs were produced by alternating fields sufficient to saturate the ARM for the particular biasing field, $H \leqslant 2000$ Oe (2000×10^{-4} T). The one exception is sample 11, which was within 10% of saturation at $H = 2000$ Oe.

sidered the thermodynamic equilibrium of an inter-
acting assemblage of uniaxial, aligned single domain
particles subject to ARM and TRM; the resulting
theory for ARM succeeds in showing in a natural
way that ARM has finite susceptibility and explains
the J_{ARM} versus h curves.

Fig. 4 summarizes the apparent grain size depen-
dence of χ_{ARM}/χ_{TRM}. The mechanism(s) responsible
for this behavior is (are) less clear. Although none of

the existing theories appear to predict this size depen-
dence of χ_{ARM}/χ_{TRM}, we shall make a plausibility
argument to show that magnetic interactions might
be responsible for the observed behavior.

The problem of how to deal with magnetic inter-
actions is extremely difficult. For simplicity's sake,
we shall approximately follow the methods of Jaep
[34], which are applicable to single-domain particles,
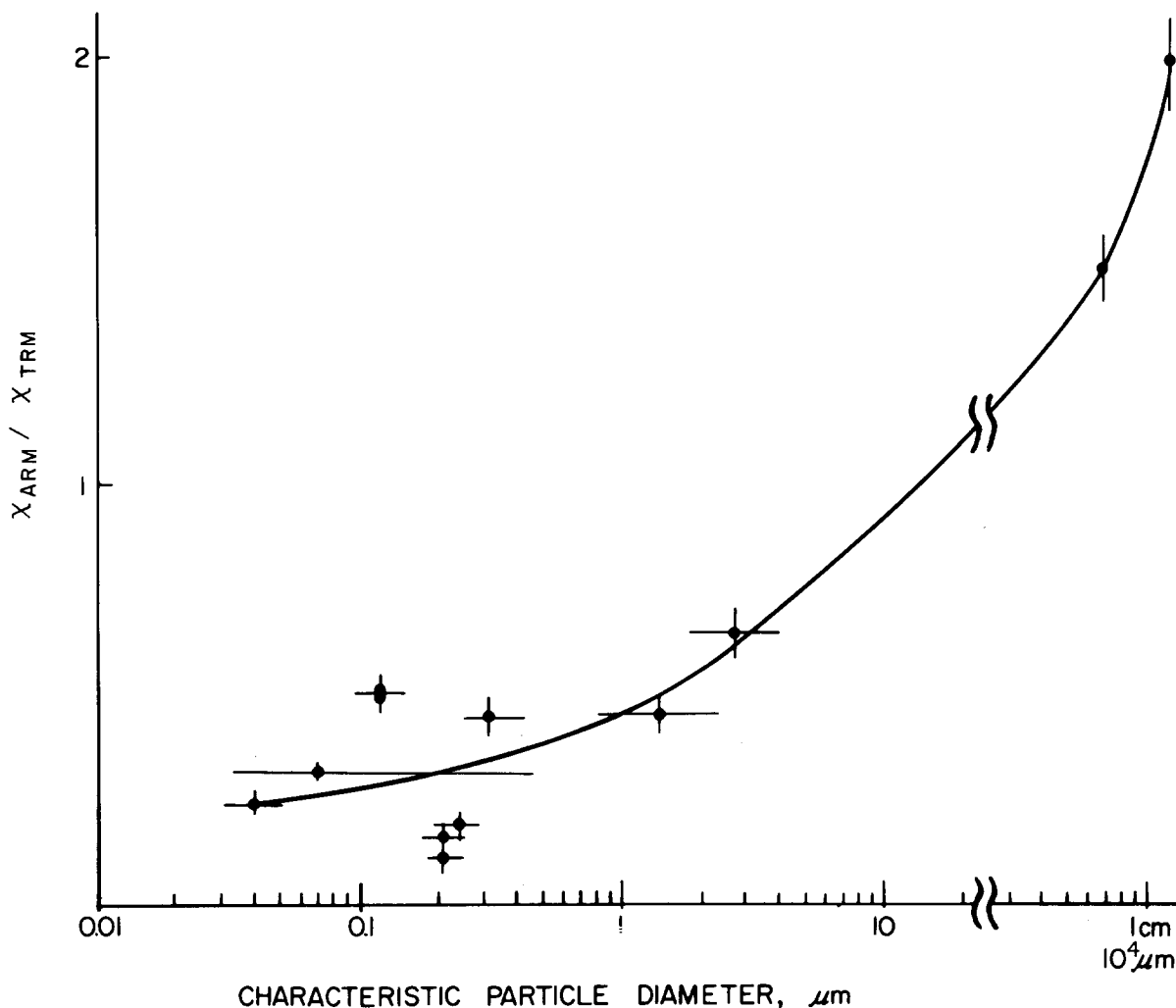to show that magnetic interactions can substantially

Fig. 4. Susceptibility ratios, χ_{ARM}/χ_{TRM}, versus particle size for the magnetite-bearing samples, samples 0 to 11. The abscissa is
identical to that of Fig. 2. The uncertainties associated with the susceptibility ratios are deviations from the mean obtained from
at least two independent measurements. Note that the susceptibility ratios are substantially below unity for submicron particles,
but they are well above unity for the large magnetite crystals.

change the χ_{ARM}/χ_{TRM} ratio. For multidomain particles the problem of magnetic interactions is much more complex because of difficulties in calculating magnetic interactions between domains present in the same grain (that is, local variations in the internal demagnetization field), as well as interactions between grains. This latter calculation can only be done after we have a better general understanding of the origin of remanence in multidomain grains.

The fact that interactions probably exist in our experimental design is inescapable, because of clustering effects present during synthesis of the samples: highly magnetic particles tend to cluster together, even though efforts were made to disperse the particles uniformly through the sample by mixing. We do not expect that clusters on the order of 10 μm or less are greatly disturbed by the mixing. We anticipate that the largest interactions between particles will generally occur in the samples with the smaller grain sizes. One exception is sample 10: in this case the sample was chemically altered to produce magnetite and significant clustering is probably absent [22].

For the region where TRM is linearly dependent on the effective field, h_{eff}, the TRM in an ensemble of identical grains can be approximated by:

$$J_{TRM} = NVJ_S(T_R)\eta\left[\frac{VJ_S h_{eff}}{kT}\right]_{blocking} \qquad (1)$$

Values inside the brackets are evaluated at the blocking temperature. In addition: V = grain volume, J_S = saturation magnetization, k = Boltzmann's constant, T = temperature, η = a constant equal to 1 in Néel's 1949 theory that relates J_{TRM} to the hyperbolic tangent of h_{eff} and is equal to 1/3 if the Langevin function is used in place of the hyperbolic tangent.

Eq. 1 differs from Néel's theory [39] in that $|\vec{h}_{eff}|$ has been substituted for the externally applied field, $|\vec{h}_{ex}|$. For a spherical sample, containing an isotropic distribution of randomly oriented magnetic grains, $|\vec{h}_{eff}|$ can be given by:

$$h_{eff} = h_{ex} - h_{int} \qquad (2)$$

Eq. 2 is supported by the observation that the experimental susceptibilities are always lower than those predicted by theories which neglect magnetic interactions. The equation also is consistent with our experiments, since the remanence is always acquired

parallel to h_{ex}, a fact that would not occur if the interaction field, h_{int}, were not aligned along the same axis as h_{ex}.

Eq. 1 can be rewritten as:

$$J_{TRM} = NVJ_S(T_R)\eta\left[\frac{VJ_S}{kT}\left(1 - \frac{h_{int}}{h_{ex}}\right)\right]_{blocking} h_{ex} \qquad (1a)$$

A similar equation can be derived for ARM [34]:

$$J_{ARM} = NVJ_S(T_R)\eta\left[\frac{VJ_S(T_R)}{kT}\left(1 - \frac{h_{int}}{h_{ex}}\right)\right] h_{ex} \qquad (3)$$

where all the parameters are to be evaluated at the temperature at which the ARM was induced, room temperature for the experiments of this study. The ratio J_{ARM}/J_{TRM} at a particular value of h_{ex} becomes, using eqs. 1a and 3:

$$\left.\frac{J_{ARM}}{J_{TRM}}\right]_{h_{ex}} = \left[\frac{J_S(T_R)T_B}{J_S(T_B)T_R}\right]\left[\frac{1 - \{h_{int}(T_R)/h_{ex}\}}{1 - \{h_{int}(T_B)/h_{ex}\}}\right] \qquad (4)$$

where we have written out explicitly the appropriate temperature dependence of J_S and h_{int}; also T_B = blocking temperature of TRM and T_R = room temperature = blocking temperature of ARM. From eqs. 1a and 3 we see that in the region where J_{ARM} and J_{TRM} are linear functions of h_{ex}, $h_{int} \propto h_{ex}$. In that region and only in that region:

$$\frac{J_{ARM}}{J_{TRM}} = \frac{\chi_{ARM}}{\chi_{TRM}} = \left[\frac{J_S(T_R)T_B}{J_S(T_B)T_R}\right]\left[\frac{1 - \lambda_{int}(T_R)}{1 - \lambda_{int}(T_B)}\right] \qquad (5)$$

where λ_{int} is a temperature-dependent, dimensionless quantity directly related to the strength of the interaction field. We can rewrite eq. 5 in the following form:

$$\frac{\chi_{ARM}}{\chi_{TRM}} = C\frac{1 - \lambda_{int}(T_R)}{1 - \lambda_{int}(T_B)} \qquad (6)$$

Because $J_S(T_R)/J_S(T_B)$ varies typically between 2 and 5 for the magnetites of this study and because values for T_R/T_B typically vary between 0.35 and 0.46, C can vary approximately between 4 and 14. As an example, if we take C = 10, $h_{int}(T_B)$ = 0 [→$\lambda_{int}(T_B)$ = 0], then for h_{ex} = 0.50 Oe (= 0.5 $\times$ 10^{-4} T) a ratio of χ_{ARM}/χ_{TRM} = 0.2 requires $h_{int}(T_R)$ = 0.49 Oe [or $\lambda_{int}(T_R)$ = 0.98]. Using an identical example as above but letting C = 1, one obtains $h_{int}(T_R)$ = 0.40 Oe [or $\lambda_{int}(T_R)$ = 0.80].

If magnetic interactions are indeed responsible for the differences between ARM and TRM acquisition [12,34,20], then ARM should become more similar to TRM when it is produced at elevated temperatures between T_R and T_B [32]. This was recently demonstrated [43] for submicron magnetite particles.

If we assume further that multidomain particles obey an equation similar to eq. [5] and if we note that generally one expects a decrease of h_{int} with change from single-domain to pseudo-single-domain to multidomain size, then the χ_{ARM}/χ_{TRM} should increase with increasing grain size, consistent with the observed behavior.

The examples given above show that if the χ_{ARM}/χ_{TRM} data are to be explained by magnetic interactions alone, then high values for $h_{int}(T_R)$, comparable to the external field, are required. That magnetic interactions are not the only cause for the low χ_{ARM}/χ_{TRM} values of the submicron magnetites is suggested by the data of sample 10. Sample 10 was prepared by reducing to magnetite the very dilute concentration of α-Fe_2O_3 that *naturally occurs* in alumina and calcium aluminate [22]. Therefore, sample 10, alone among our samples, should be free of magnetite powder agglomeration and its magnetic grains should be most uniformly dispersed and its interaction field due to neighboring grains should be less than for any of the samples containing submicron magnetites. Sample 10 also has the lowest sample demagnetizing field of all samples studied, being less than 1% of that of sample 11 (see Table 1). Therefore sample 10 should be the least influenced by magnetic interactions. Still, sample 10 has a low χ_{ARM}/χ_{TRM} value of 0.31, for which numerical calculations as in the above examples would require interaction fields in excess of 0.4 Oe, not significantly lower than for other samples containing submicron magnetite which are known to be more susceptible to the influences of magnetic interactions. This leaves us with an uneasy feeling as to the correctness of the above interaction arguments, which compare directly the acquisition of ARM and TRM. It might be that, although magnetic interactions are indeed responsible for differences in ARM of certain samples and differences in the TRM of certain samples, the direct comparison of ARM and TRM acquisition might not be valid due to fundamental differences in their acquisition.

8. Conclusions

The question may arise as to whether the apparent grain size effect on intensity is real or whether it is coincidental owing to a systematic increase in magnetic interactions between particles with decrease in mean grain sizes. That this is not the case can be seen by reflecting on the data of Table 1, and in particular on the data of sample 10, which by the discussion of the last section should be least influenced by magnetic interactions, yet its value for χ_{ARM}/χ_{TRM} = 0.31. Therefore, the gross trend of the behavior of χ_{ARM}/χ_{TRM} as drawn in Fig. 4 is in large part related directly to the particle sizes, possibly through the grain's own demagnetizing field. The variations in Fig. 4 for the submicron grain sizes might be in part caused by different interaction fields of the samples due to variations in particle agglomerations, particle shapes and spontaneous magnetization. In addition, the χ_{ARM}/χ_{TRM} result for sample 10 might represent a measure of the fundamental difference between ARM and TRM in the presence of little or no magnetic interactions.

The difference in the susceptibility ratios of samples 6 and 7 probably reflects the relative importance of the sample demagnetizing effect on the acquisition of ARM, because samples 6 and 7 differ only in their concentration of magnetite powder, sample 7 having 1.4% magnetite by weight as opposed to the 0.14% for sample 6. Since both samples contain the same species of magnetite particles (mean diameter of 0.21 μm) and because we do not expect that particle clusters of the order of 10 μm or less are greatly disturbed by the mixing during sample preparation, samples 6 and 7 should have the same interaction effects due to near neighbors and due to the grains' self-demagnetization.

The stabilities of ARM and TRM appear to be very similar with respect to AF demagnetization, low-temperature cycles and spontaneous decay in zero field at room temperature. Part of the reason for this remarkable similarity must result from the experimental design in which we restricted our experiments to samples that individually do not display a large distribution of particle sizes. This follows from our observations that χ_{ARM}/χ_{TRM} strongly increases with grain size increase. ARM in a rock containing multidomain and single-domain grains should be somewhat less stable magnetically with respect to AF demag-

netization than a TRM. In the few cases where rock samples have been studied [40,41], the AF demagnetization curves of ARM and NRM, which is presumably a TRM, are remarkably similar, suggesting that in these cases the NRM is also carried by a relatively narrow range of particle sizes.

We note that small (pseudo-single domain and/or single domain) grains are believed to carry most of the stable remanence in a typical rock. The variation in stability of such grains with changes in grain size usually appears to be much smaller than the variations in χ_{ARM}/χ_{TRM} (Table 1). Therefore, samples with very similar ARM and TRM stabilities, as measured by AF demagnetization, may exhibit very different ARM to TRM intensity ratios. Although it may often be reasonable to use ARM to model TRM, in so far as the stabilities of the remanence are concerned, its use in some paleointensity techniques should be viewed with skepticism. For example, the ARM paleointensity techniques [19,20] used on lunar samples do not seem to give very good control over potential errors due to variations in grain size. In particular, if iron shows similar grain size variations, then it is not clear that the alleged decrease in lunar paleointensity with age [19] is resolvable by the ARM method used to obtain the paleointensity values.

Acknowledgements

References

1 L. Néel, Cahiers Phys. 12 (1942) 2.
2 L. Néel, Cahiers Phys. 13 (1943) 18.
3 L. Néel, Cahiers Phys. 17 (1943) 47.
4 L. Néel, R. Forrer, N. Janet and R. Baffie, Cahiers Phys. 17 (1943) 51.
5 L. Lliboutry, Ann. Phys. 6 (1951) 731.
6 E. Thellier and F. Rimbert, C.R. Acad. Sci., Paris 239 (1954) 1399.
7 F. Rimbert, Rev. Inst. Fr. Pétrole 14 (1959) 123.
8 F. Preisach, Z. Phys. 94 (1935) 277.
9 J.G. Woodward and E. Della Torre, J. Appl. Phys. 31 (1960) 56.
10 E.D. Daniel and I. Levine, J. Acoust. Soc. Am 32 (1960) 1.
11 B.J. Patton and J.L. Fitch, J. Geophys. Res. 67 (1962) 307.
12 D.J. Dunlop and G.F. West, Rev. Geophys. Space Phys. 7 (1969) 709.
13 H.P. Johnson and R.T. Merrill, J. Geophys. Res. 77 (1972) 334.
14 H.P. Johnson and R.T. Merrill, J. Geophys. Res. 78 (1973) 4938.
15 H.P. Johnson and R.T. Merrill, J. Geophys. Res. 79 (1975) 5533.
16 H.P. Johnson, H. Kinoshita and R.T. Merrill, Geol. Soc. Am. Bull. 86 (1975) 412.
17 S. Levi and S.K. Banerjee, Earth Planet Sci. Lett. 29 (1976) 219.
18 H. Markert and F. Heller, Phys. Stat. Solidi, A 14 (1972) K47.
19 A. Stephenson and D.W. Collinson, Earth Planet Sci. Lett. 23 (1974) 220.
20 S.K. Banerjee and J.P. Mellema, Earth Planet. Sci. Lett. 23 (1974) 177.
21 J. Shaw, Geophys. J.R. Astron. Soc., London 39 (1975) 133.
22 S. Levi and R.T. Merrill, submitted to J. Geophys. Res. (1976).
23 K.J. Gallagher, W. Feitknecht and U. Mannweiler, Nature 217 (1968) 1181.
24 R.T. Merrill, Geophys. Surv. 2 (1975) 277.
25 M. Ozima, M. Ozima and T. Nagata, J. Geomagnet. Geoelectr. 16 (1964) 37.
26 M. Ozima, M. Ozima and S. Akimoto, J. Geomagnet. Geoelectr. 16 (1964) 165.
27 K. Kobayashi and M.D. Fuller, Philos. Mag. 18 (1968) 601.
28 R.T. Merrill, J. Geophys. Res. 75 (1970) 3343.
29 F.D. Stacey and S.K. Banerjee, The Physical Principles of Rock Magnetism (Elsevier, Amsterdam 1974) 195 pp.
30 D.J. Dunlop and E.D. Waddington, Earth Planet. Sci. Lett. 25 (1975) 11.
31 M.E. Bailey and D.J. Dunlop, EOS Trans. Am. Geophys. Union 56 (1975) 975 (abstract).
32 S. Levi, Ph.D. Thesis, Univ. of Washington (1974) 210 pp.
33 D.E.W. Gillingham and F.D. Stacey, Pure Appl. Geophys. 8 (1971) 160.
34 W.F. Jaep, J. Appl. Phys. 42 (1971) 2790.
35 D.F. Eldridge, J. Appl. Phys. 32 (1961) 2475.
36 E.P. Wohlfarth, J. Appl. Phys. 35 (1964) 783.
37 R.K. Waring, J. Appl. Phys. 33 (1967) 1005.
38 E. Kneller, J. Appl. Phys. 39 (1968) 945.
39 L. Néel, Ann. Géophys. 5 (1949) 99.
40 J.K. Park and E. Irving, Can. J. Earth Sci. 7 (1970) 1499.
41 J. Brooke, E. Irving and J.K. Park, Can. J. Earth Sci. 7 (1970) 1515.
42 V.A. Schmidt, Earth Planet. Sci. Lett. 20 (1973) 440.
43 D.J. Dunlop, M.E. Bailey and M.F. Westcott-Lewis, Proc. 6th Lunar Sci. Conf., Geochim. Cosmochim. Acta., Suppl. 6, 3 (1975).